J.Natn.Sci.Foundation Sri Lanka 2023 51 (3): 399 - 413
DOI: http://dx.doi.org/10.4038/jnsfsr.v51i3.11221

RESEARCH ARTICLE

Cosmeceutics

pH-dependent release properties of curcumin encapsulated alginate nanoparticles in skin and artificial sweat

IF Shakoor[1], GK Pamunuwa[1*] and DN Karunaratne[2]

[1] *Department of Horticulture and Landscape Gardening, Faculty of Agriculture and Plantation Management, Wayamba University of Sri Lanka, Makandura, Gonawila, Sri Lanka.*

[2] *Department of Chemistry, Faculty of Science, University of Peradeniya, Peradeniya, Sri Lanka.*

Submitted: 03 June 2022; Revised: 26 December 2022; Accepted: 24 February 2023

Abstract: Topical skin application of curcumin is challenging due to the low solubility and poor stability, including fast photodegradation, of this bioactive compound. Therefore, curcumin encapsulated alginate (CU-Al) nanoparticles were prepared by the ionic gelation method followed by freeze drying to determine the efficacy of alginate in facilitating curcumin release. Evaluation of the release of curcumin from the encapsulate in the presence of artificial sweat (pH 4.7) and skin (pH 5.5), about which the literature is meagre, was carried out after particle size characterization. CU-Al nanoparticles were in the nano-range (186.8 nm), assimilated a negative zeta-potential value (-15.4 ± 8.13 mV), and displayed a high encapsulation efficiency (94.55 ± 0.53%). The release of encapsulated curcumin at pH 5.5 (max. 64%) and at pH 4.7 (max. 27%) were significantly different. In pH 5.5 and pH 4.7, the release profiles of encapsulated curcumin fitted best with the Weibull (followed an anomalous transport mechanism) and Gompertz (followed a super case II transport mechanism) models respectively, displaying sigmoidal release patterns. Diffusion and polymer relaxation/swelling based release at pH 5.5 and rapid polymer relaxation/erosion based release at pH 4.7 have governed the encapsulated curcumin release. The results indicated that CU-Al nanoparticles may be utilized to facilitate controlled and prolonged release of curcumin in both skin and artificial sweat, thereby functioning as a promising novel delivery vehicle for curcumin. However, skin deposition or penetration may be required for yielding a satisfactory topical administration of curcumin during sweating.

Keywords: Alginate polymer, curcumin, nanoparticle formulation, release kinetic mechanisms, skin delivery.

INTRODUCTION

Skin, as a sensitive organ and as the first line of defence, is very susceptible to injuries, burns, infections, rashes, acne, and skin related disorders such as scleroderma, dermatitis, psoriasis, etc. (Chanchal & Swarnlata, 2008). Exposure to sunlight (UV radiation) and various other environmental conditions could lead to photo-aging, damaging and darkening of skin, and skin cancer problems (Svobodová *et al*., 2003; Afaq & Mukhtar, 2006; Thangapazham *et al*., 2013). As a remedy for the aforementioned skin related issues, development of cosmetic products in the form of nano-cosmetics has emerged (Boonme *et al*., 2009; Saraf & Kaur, 2010; Li *et al*., 2011; Taib *et al*., 2015).

Curcumin, which is a polyphenolic phytoconstituent derived from the rhizome of turmeric (*Curcuma longa*), has been utilized in skin formulations since ancient times. Curcumin possesses antibacterial, anti-oxidant, anti-inflammatory, antifungal, antiproliferative, anti-viral, anticancer, and wound healing properties that are highly beneficial in addressing skin related issues. Moreover, curcumin acts as a protective agent against various chemicals and environmental pollutants that could cause skin damage (Thangapazham *et al*., 2013). Regardless of the high functionality of curcumin, its poor solubility (Dutta & Ikiki, 2013), fast photodegradation upon exposure to sunlight (Tønnesen *et al*., 1986; Lee *et al*., 2013a), low bioavailability (Dutta & Ikiki, 2013) and poor stability in neutral and alkaline aqueous solutions and in hydrophilic topical formulations (Guadarrama-Acevedo *et al*., 2019) could be considered as major drawbacks that make its direct application challenging.

[*] Corresponding author (geethip@wyb.ac.lk; https://orcid.org/0000-0002-1156-5088)

In the recent past, many studies have been conducted to enhance the properties of curcumin for topical and transdermal delivery using alginate (Guadarrama-Acevedo *et al*., 2019), chitosan (Nair *et al*., 2019), nanoliposomes (Zhao *et al*., 2013), and solid lipid nanoparticles (Rungphanichkul *et al*., 2011; Zamarioli *et al*., 2015). Also, numerous topical formulations of curcumin have been developed and investigated for wound healing over the past years. For example, the review by Kumari *et al*. (2022) highlights the usage of different curcumin loaded nanocarriers such as liposomes, nanoparticles, nanoemulsions, quantum dots, lipid nanoparticles and polymeric micelles, and other polymeric systems of curcumin for wound healing.

Although such systems undoubtedly improve skin permeation and distribution of loaded bioactives, the mechanism by which this enhancement is achieved is unclear. When developing topical formulations, it is important to understand the effect of numerous variables including pH on the penetration and permeation of bioactives through the skin (de Oliveira *et al*., 2021). Current research on topical formulations of curcumin appears promising. However, the majority of published evidence is based on *in vitro* release in phosphate buffered saline (PBS) pH 7.4 or skin pH 5.0 with *ex vivo* skin permeation studies (Pamunuwa *et al*., 2016; Sharma *et al*., 2020). Yet, the effect of sweat on the release of curcumin has been poorly investigated. Specifically, the release of curcumin in the absence of sweat (at skin pH 5.5) and in the presence of sweat (pH 4.7) from alginate nanoparticles pertinent for cosmetic formulations has not been studied so far or has been rarely evaluated, although alginate and curcumin are frequently investigated for skin applications (Zakerikhoob *et al*., 2021; Kumari *et al*., 2022; Sahu & Mallick, 2022). However, gaining an understanding of the release mechanism of encapsulated curcumin, especially during sweating, is very important in order to comprehend the skin penetration ability and longevity of bioactive agents once administered topically.

For this purpose, alginate (derived from seaweed) was utilized in this study to formulate curcumin encapsulated nanoparticles which were then evaluated for release properties in media pertinent to skin. Biodegradability, biocompatibility, and non-toxicity, along with other remarkable properties of alginate beneficial for skin application, were considered in selecting this matrix. Hydrophilicity, high absorption capacity, haemostatic nature, swelling and gelling capabilities, ability to be crosslinked, bio similarity to extracellular matrices, controllable porosity, bio adhesivity, and affordability, which are properties of alginate important in wound healing, are beneficial for skin applications as well (Aderibigbe & Buyana, 2018; Guadarrama-Acevedo *et al*., 2019; Sahu & Mallick, 2022).

After characterizing the freeze-dried curcumin encapsulated alginate particles for encapsulation efficiency, loading capacity, particle size, polydispersity index, zeta-potential, and morphology, *in vitro* release at skin pH 5.5 and in artificial sweat (pH 4.7) was carried out for release model fitting and elucidation of the release mechanism, which have not been reported previously. Importantly, the release model of best fit for the release profiles and the release transport mechanism of curcumin from the nanoparticle system were determined to obtain a thorough understanding of the release of curcumin from alginate nanoparticles in media pertaining to skin conditions. The findings of this study may contribute to the development and formulation of curcumin encapsulated nano-cosmetic formulations.

MATERIALS AND METHODS

Materials

Curcumin (≥ 65% purity), sodium alginate, sorbitan monooleate (Span 80) and dialysis tubing cellulose membrane (avg. flat width 43 mm/12,000 MWCO) were purchased from Sigma Aldrich Company (St. Louis, MO, USA). All other chemicals were of analytical grade.

Synthesis of curcumin encapsulated alginate (CU-Al) nanoparticles

Curcumin encapsulated alginate (CU-Al) nanoparticles were prepared using the ionic gelation method followed by centrifugation and freeze drying as described by Pamunuwa *et al*. (2021) with modifications as follows.

Initially, alginate (1.0 g) was dissolved in distilled water in order to obtain a solution of 1.0% (w/v) and the pH was adjusted to 5. After stirring the solution, span 80 (0.4% v/v) was added to the solution which was then

stirred for 2 h. Next, 5 mg of curcumin (CU) dissolved in ethanol (5 mL) was added to the solution, which was stirred well to obtain a homogeneous solution. Then, 50 mL of $CaCl_2$ (1.5% w/v) was added dropwise as a crosslinker to the mixture and stirring was continued for 1 h. Finally, the solution was refrigerated overnight, and was then centrifuged (12, 000 RPM for 45 min) and freeze dried to obtain a free-flowing powder of CU-Al nanoparticles. The stirring speed and the temperature of the solution were maintained at 1200 RPM and 60 ºC, respectively, throughout the study. Plain alginate particles were prepared similarly without incorporating CU. All the experiments were carried out under dark conditions.

Determination of encapsulation efficiency (% EE) and loading capacity (% LC)

EE and LC (%) were determined by measuring absorbance at wavelength (λ_{max}) 425 nm using a UV-Vis spectrophotometer (Evolution 220 / Thermo Fisher Scientific, USA). The amount of CU in the supernatants obtained by centrifuging the particle suspensions was determined. The experiments were carried out in triplicate under dark conditions.

% EE and % LC were calculated using the equations (1 and 2) shown below, respectively (Pamunuwa *et al*., 2016).

$$\% \text{ EE} = \frac{\text{Mass of total amount of CU used} - \text{Mass of CU in supernatant}}{\text{Mass of total amount of CU used}} \times 100 \quad \ldots(01)$$

$$\% \text{ LC} = \frac{\text{Mass of CU entrapped}}{\text{Mass of particles used}} \times 100 \quad \ldots(02)$$

where, CU stands for curcumin.

Particle characterization

Determination of particle size (D_{50}), polydispersity index (PDI) and zeta- potential

The particle size of CU-Al particles dispersed in distilled water was measured using a particle size analyzer (Cilas Nano DS, France). The dynamic light scattering (DLS) technique was utilized in order to obtain the particle size and the PDI of the particles. The zeta-potential of CU-Al particles dispersed in distilled water was measured using a Zeta-Potential Analyzer (Zetasizer Nano ZS, Malvern Instruments, UK) that uses the laser doppler electrophoresis technique.

Fourier transform infrared spectroscopy (FTIR) analysis

Infrared spectra of free CU, freeze dried free alginate nanoparticles and CU-Al nanoparticles were obtained in the range of 500-4000 cm^{-1} wavenumber under the absorbance mode, using the attenuated total reflection (ATR) (Alpha, Bruker, Germany) technique in order to verify the encapsulation of CU in the alginate matrix.

Scanning electron microscopic (SEM) imaging

To evaluate the surface morphology of the CU-Al nanoparticles, freeze dried CU-Al nanoparticles were scanned using SEM (ZEISS EVO/LS15). Nanoparticles were sprinkled on a conductive double adhesive tape supported by an aluminum stub followed by gold sputtering. Finally, the sample was scanned with an acceleration voltage and a magnification of 5.0 kV and 50.00 K X, respectively, to obtain a SEM image.

***In vitro* release study at skin pHs**

In vitro release of CU from alginate nanoparticles at the average skin pH of 5.5 and artificial sweat pH of 4.7 was carried out as described by previous studies using the dialysis bag method (Pamunuwa *et al*., 2015; Ariyarathna & Karunaratne, 2016) with slight modifications as follows.

First, a known quantity of CU-Al nanoparticles was suspended in pH 5.5 phosphate buffer solution (10 mL) in a dialysis bag which was then submerged in the same buffer solution (100 mL). The temperature of the medium and the speed of stirring were maintained at 37 ± 2 °C and 400 RPM, respectively, throughout the 8 h of release study. Next, an aliquot from the release medium was removed to quantify the amount of CU at one-hour intervals. The release medium was replenished with the same volume of fresh buffer solution each time an aliquot was removed. The amount of CU released was determined using a UV-Vis spectrophotometer by measuring the absorbance at 421.1 nm wavelength (pH 5.5 λ_{max} = 421.1 nm). A similar study was carried out using artificial sweat of pH 4.7 as the release medium (pH 4.7 λ_{max} = 437.1 nm). Also, parallel experiments were carried out using free CU.

The cumulative release percentage was calculated by using the following equation (3) (Ariyarathna & Karunaratne, 2016).

$$\text{Cumulative release (\%)} = \frac{\text{Total amount of CU released to the medium}}{\text{Total encapsulated CU used}} \times 100 \quad \ldots(3)$$

where, CU stands for curcumin.

Phosphate buffer of pH 5.5 (European Pharmacopoeia 7.0) and artificial sweat (Randin, 1987; Pamunuwa *et al*., 2015) of pH 4.7 were prepared according to the procedures stated briefly as follows.

Phosphate buffer solution: 96.4 mL of KH_2PO_4 (13.61 g L^{-1}) was mixed with 3.6 mL of Na_2HPO_4 (35.8 g L^{-1}) and the solution was diluted to 1 L using distilled water.

Artificial sweat solution: NaCl (20 g), NH_4Cl (17.5 g), urea (5 g), acetic acid (2.5 g) and *d,l*-lactic acid (15 g) were added to 1 L of distilled water and pH of the solution was brought to 4.7 using $NaOH_{(aq)}$.

Release model fitting and transport mechanism

The data of CU release from CU-Al nanoparticles were fitted into different drug release kinetic models (Dash *et al*., 2010; Pamunuwa *et al*., 2020) to determine the kinetic model of best fit and the release transport mechanisms of CU. The model with the highest R-square value was considered as the model of best fit. The equations (equations 4-10) of the release kinetic models are indicated below.

Zero Order: $Q_t = Q_0 + K_0\, t$ …(4)

where, Q_t - Amount of curcumin (CU) dissolved in time t
Q_0 - Initial amount of CU in the solution
K_0 - Zero order release constant

First Order: $\log C = \log C_0 - Kt/2.303$ …(5)

where, C_0 - Initial concentration of curcumin (CU)
C - Concentration of CU at time t
K - First order rate constant

Higuchi: $Q_t = K_H \times t^{1/2}$ … (6)

where, Qt - Amount of curcumin (CU) released in time t
K_H - Higuchi dissolution constant

Hixson-Crowell: $M_0^{1/3} - M_t^{1/3} = \kappa_{HC}\, t$ …(7)

where, M_0 - Initial amount of curcumin (CU) in the matrix
M_t - Remaining amount of CU in the matrix at time t
κ_{HC} - Hixson-Crowell constant

Baker-Lonsdale: $f = \frac{3}{2}\left[1 - (\frac{M_t}{M_\alpha})^{2/3}\right] - \frac{M_t}{M_\alpha} = kt$ …(8)

where, M_t/M_α - Fraction of curcumin (CU) released at time t
k - Release constant

Weibull: $M = M_0\,[1 - e^{\left\{-\frac{(t-T)^b}{a}\right\}}]$ …(9)

where, M - Amount of curcumin (CU) dissolved as a function of time t
M_0 - Total amount of CU being released
T - Lag time
b - Shape parameter
a - Scale parameter

Gompertz: $X(t) = X_{max} x\, e^{\{-\alpha\, e^{\beta \log t}\}}$ …(10)

where, $X(t)$ - Percentage of curcumin (CU) dissolved at time t
X_{max} - Maximum dissolution
α - Undissolved proportion at time t (location/scale parameter)
β - Dissolution rate per unit of time (shape parameter)

To evaluate the release transport mechanisms of the release of CU from CU-Al nanoparticles at pH 5.5 and pH 4.7, the semi-empirical model 'Power Law' (equation 11) described by Korsmeyer *et al*. (1983) was utilized.

$$\frac{M_t}{M_\infty} = \kappa t^n \quad \text{…(11)}$$

where, M_t / M_∞ is the fraction of curcumin (CU) released at time t, κ is the release rate constant and n is the diffusional exponent.

The diffusional exponent (n) for each trial was determined by fitting the first 60% of the CU release data in the linearized power law equation (equation 12) which is shown below to obtain a linear plot of $M_t/M_\infty \leq 0.6$ versus log t.

$$log\left(\frac{M_t}{M_\infty}\right) = log\,\kappa + n\,log\,t \quad \text{…(12)}$$

where, Mt / M∞ is the fraction of curcumin (CU) released at time t, κ is the release rate constant and n is the diffusional exponent.

Next, the release transport mechanisms of CU-Al nanoparticles showing spherical shaped geometry were evaluated based on different (n) values obtained for the release of CU from CU-Al nanoparticles at pH 5.5 and pH 4.7. The n values corresponding to different release mechanisms are stated in Table 1 (Korsmeyer *et al*., 1983; Peppas & Sahlin, 1989; Azad *et al*., 2020).

Table 1: Diffusional exponent ('n') values from power law corresponding to different release mechanisms for spherical particles

'n' value (Diffusional Exponent)	Release mechanism
n < 0.43	Quasi – Fickian (diffusion controlled release)
n = 0.43	Fickian (diffusion controlled release)
0.43 < n < 0.85	Anomalous transport-non Fickian diffusion (diffusion and polymer relaxation controlled release)
n = 0.85	Case II transport mechanism (release based on relaxation of the polymeric chains or swelling)
n > 0.85	Super case II transport mechanism (release based on polymer chain expansion or relaxation)

Statistical analysis

All data are presented as mean ± standard deviation (SD) of parallel experiments. Origin 6 and Origin Pro (9.1) software were used for curve fitting. One-way ANOVA with a significance value of $p \leq 0.05$ was carried out using Minitab 16 software. Microsoft Office Excel (2010) was used for producing graphs.

RESULTS AND DISCUSSION

Synthesis of CU-Al nanoparticles

Synthesis of CU-Al nanoparticles was completed successfully by using the ionic gelation method, which is one of the most common methods of alginate hydrogel preparation (Kim *et al*., 2000). The utilization of the ionic gelation method under very mild conditions has avoided any toxic chemical involvements (Usmiati *et al*., 2014) during nanoparticle preparation, making these particles safe for topical use. Also, enhanced protection from light and temperature may be provided to CU by encapsulation in alginate according to another study carried out by our group (Shakoor *et al*, 2023).

%EE and %LC

Encapsulation of CU in alginate displayed a high %EE of 94.55 ± 0.53% and was similar to those values reported in the literature (Nguyen *et al*., 2015). However, the %LC was moderate and was 0.47 ± 0.00%. The reason for obtaining only a moderate loading capacity may be the utilization of low CU to alginate ratio (Ji *et al*., 2012). However, the increment of the amount of CU further led to adsorption of CU on the surface of the alginate polymer which in turn may lead to higher agglomeration of the particles. Therefore, the CU to alginate ratio was maintained at 1:200 (w/w) to enhance encapsulation and avoid/reduce adsorption of CU on the surface of alginate particles.

Particle size, PDI and zeta-potential

The stratum corneum (SC), which is the outermost layer of the epidermis of the skin, acts as a barrier against the penetration of numerous substances, including therapeutic formulations, through the skin (Kim *et al*., 2020). The size of the particles usually has an influence on skin barrier penetration, and thus particle size determination of formulations designed for topical application is mandatory (Uchechi *et al*., 2014). Explicitly, the smaller the particles become, the easier it is for deep skin infiltration (Hoet *et al*., 2004). In this study, the median (D50) value of the hydrodynamic diameter of CU-Al nanoparticles was 186.8 nm. The utilization of $CaCl_2$ as a crosslinker along with Span 80 as a non-ionic surfactant may have affected the particle size (Paradee *et al*., 2012; Suhail *et al*., 2019). Evidently, biopolymeric nanoparticles tend to have low stability leading to a broad particle size distribution via agglomeration. However, crosslinking increases the stability of nanoparticles while decreasing particle agglomeration (Paradee *et al*., 2012; Suhail *et al*., 2019). Figure 1 shows the distribution of the particle size (hydrodynamic diameter) of the CU-Al nanoparticles in aqueous medium.

It is highlighted in the literature that nanocarriers developed for cosmetics or dermatology need to be sufficiently small to allow efficient penetration in to the skin owing to their high surface area and mechanical strength (Nguyen *et al*., 2015). Nanoparticles with diameters below 500 nm guarantee direct contact with the stratum corneum due to their larger surface area to volume ratio. Therefore, CU-Al particles of nano size are expected to enhance dermal permeation, as a result of skin barrier passage including intracellular passage, making it more appropriate for topical application (Krausz *et al*., 2015; Guadarrama-Acevedo *et al*., 2019). However, the particles should not be too small since they tend to diffuse into the blood stream. Also, particles of diameter ~200 nm have been considered suitable for topical applications (Nguyen *et al*., 2015). Thus, it is clearly evident that the particle sizes obtained in this study are suitable for skin delivery. Try *et al.* (2016) showed, using nanocarriers of two different sizes (*i.e.*, 70 nm and ~300 nm), that particles of sizes in this range exhibit skin penetration and that the depth of skin penetration of the smaller particles is greater than that of larger particles. Hence, CU-Al particles fabricated in this study may show skin penetration, in addition to release of CU, on topical application.

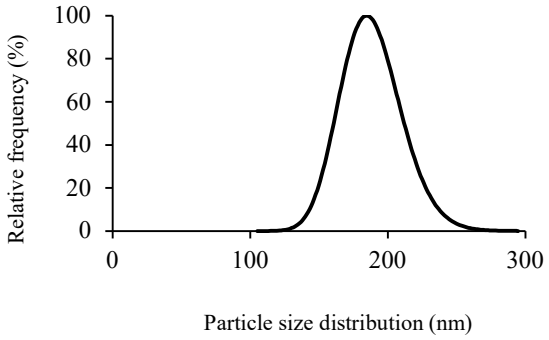

Figure 1: Particle size distribution of CU-Al nanoparticles in aqueous medium

The PDI value of the CU-Al nanoparticles was 0.292 which suggests a monodispersed and uniform distribution of particle size which is favorable for developing skin formulations. In the case of a polymeric nanoparticle system, maintaining the PDI value as low as possible (≤ 0.2) is important to obtain a monodispersed particle size distribution (Danaei *et al*., 2018).

The zeta-potential value of CU-Al nanoparticles was -15.4 ± 8.1 mV, indicating an incipient instability in aqueous medium. Zeta potential values around -30 mV generally ensure colloidal stability due to strong electrostatic repulsion between the nanoparticles (Nguyen *et al*., 2015). Yet, according to the literature, a zeta potential of -10 mV could be adequate in order to maintain the stability of nano-systems in suspensions (Nguyen *et al*., 2015). According to the zeta-potential reported in this study, -15.4 ± 8.1 mV, the fabricated CU-Al particles may show only incipient instability, and may exhibit adequate stability for the development of a skin formulation. Interestingly, charged drug carriers have caused increased diffusion of the drugs through the skin. Further, negatively charged carriers have shown a higher flux of drugs than positively charged carriers in numerous instances (Sinico *et al*., 2005; Lee *et al*., 2013b). Also, electrostatic interactions between the positively charged nanoparticles with negatively charged molecules in the matrix have caused a slowing down of particle diffusion (Lee *et al*., 2013b). However, the influence of nanoparticle charge on skin permeation is quite inconsistent according to the literature.

Overall, improved skin permeation, while protecting the encapsulated bioactive compound, may be expected according to the particle size, PDI, and zeta potential of CU-Al nanoparticles synthesized in this study.

FTIR analysis

Evaluation of the functional groups of pure CU, lyophilized plain alginate nanoparticles, and CU-Al nanoparticles was carried out by using FTIR-ATR technique, in order to confirm the interactions of the alginate polymer matrix with CU in CU-Al nanoparticles. Figure 2 displays the FTIR spectra of free CU, freeze dried alginate and CU-Al nanoparticles.

The characteristic peaks of the IR spectrum of pure CU closely aligned with the literature values (Ismail *et al*., 2014; Chen *et al*., 2015; Pecora *et al*., 2016; Okagu *et al*., 2020). A prominent broad peak corresponding to the stretching vibrations of phenolic OH groups at 3504.6 cm^{-1}, sharp narrow peaks corresponding to aromatic C=C stretching vibrations at 1507.2 cm^{-1} and C=O stretching of the keto group at 1626.7 cm^{-1} were observed. Peaks at 1274.2 cm^{-1} and 1424.9 cm^{-1} corresponding to the C-O stretching vibration of phenolic group and bending vibration of C-H (alkane), respectively, were also observed. In addition, the peak at 1231.3 cm^{-1} is attributable to asymmetric C-O-C stretching vibrations, while the peak at 1025.4 cm^{-1} is attributable to symmetric C-O-C stretching vibrations. The characteristic peaks at 856.9 cm^{-1} and 809.2 cm^{-1} represent the C-H out of plane bending mode of the meta- and para-substituted aromatic moiety.

Encapsulation of CU in alginate has caused shifting of certain peaks and revealed the distinct absorption peaks of CU indicating a mixture of signals in the spectrum of CU-Al particles. The shifting of the peaks of alginate on encapsulation of CU is indicated in Table 2 (Nastaj *et al*., 2010; Larosa *et al*., 2018).

Table 2: Shifted FTIR peaks of plain alginate and curcumin encapsulated alginate nanoparticles

Vibration/ functional group	Peak (cm^{-1})	
	Alginate	CU-Al nanoparticles
Stretching vibrations of O-H group (broad peak)	3267.7	3259.5
Stretching vibrations of aliphatic C-H	2923.9	2921.8
Shoulder peak corresponding to the stretching vibrations of the C-O group of the un-dissociated carboxylic group	1737.8	1746.1
Splitting of COO- stretching into asymmetric C=O vibrations	1412.5	1418.6
C-O stretching vibrations	1299.3	1293.1
C-O, C-C, and COC stretching vibrations	1085.3	1081.0
C-C and COC vibrations	1029.5	1025.4

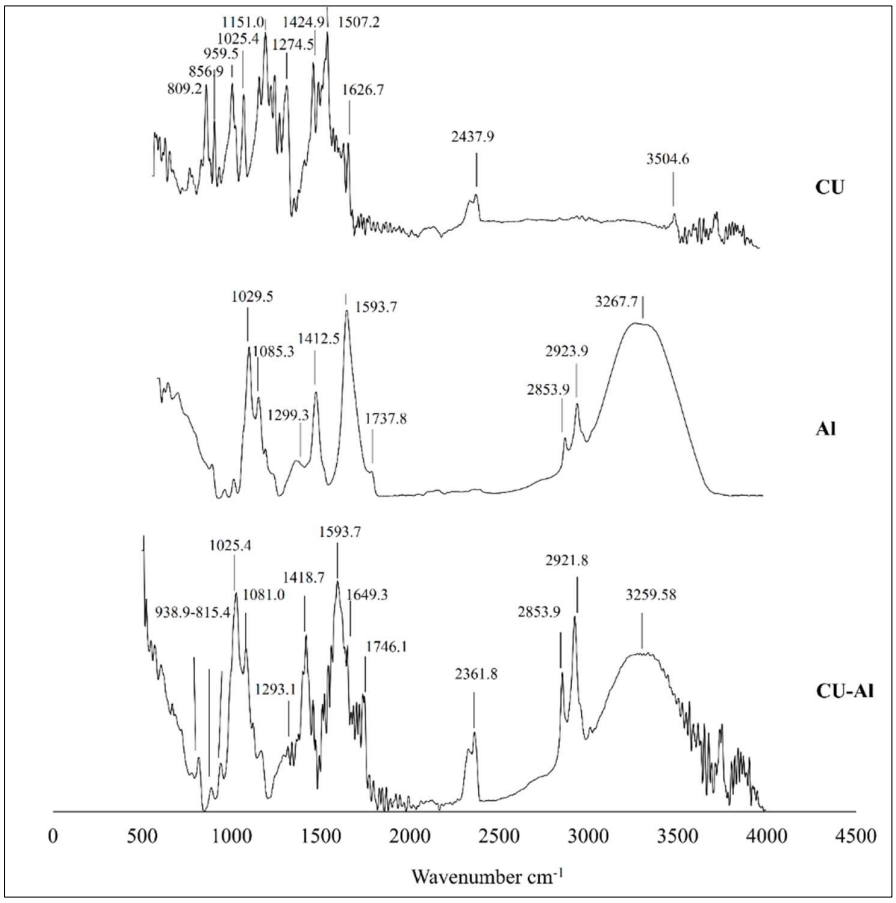

Figure 2: FTIR of pure CU, freeze dried alginate and CU-Al nanoparticles, respectively. (CU : curcumin, Al : Alginate, CU-Al : Curcumin encapsulated alginate particles)

Further, especially, the appearance of characteristic peak of pure CU at 2437.9 cm^{-1} in the functional group region of CU-Al nanoparticles at 2361.8 cm^{-1} and the observation of peaks related to pure CU in the finger print region of CU-Al encapsulate indicated that the CU was loaded into the alginate matrix of the nanoparticles successfully.

SEM Imaging

Figure 3 shows the SEM image of freeze-dried CU-Al nanoparticles. According to the SEM image, CU-Al nanoparticles displayed a spherical shape and diameters mostly below 200 nm. As expected, the diameter of the freeze-dried particles was smaller than the hydrodynamic diameter. Even though the homogeneity of CU-Al particle sizes is not clear in the SEM image, obtaining a single peak in DLS data close to 186 nm proved a uniform particle size distribution. However, the appearance of lump structure in the background of the SEM image may be probably due to agglomeration and cluster formation of the freeze-dried particles during the time of sample preparation. Depending on the type of skin formulation, either freeze dried particles or wet particles may be used since the particle size may have a significant influence on the efficacy of the skin formulation (Uchechi *et al*., 2014).

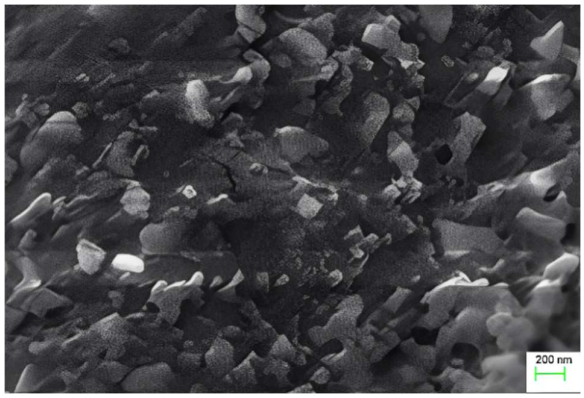

Figure 3: SEM image of CU-Al particles (CU-Al : Curcumin encapsulated alginate)

In vitro release of CU from CU-Al nanoparticles at skin pHs

An *in vitro* release study was performed to determine the release models and mechanisms of release of CU from CU-Al nanoparticles at average skin pH 5.5 and in sweat at pH 4.7. Figure 4 shows the comparative release of free CU and CU from CU-Al nanoparticles at pH 5.5 and in artificial sweat.

At pH 5.5, release of free CU was significantly higher than that from the CU encapsulated nanoparticles. Free CU displayed a burst release of around 40% during the very first hour of the release time. The highest release of free CU was approximately 93%. However, release of CU from CU-Al nanoparticles displayed a much controlled and slower release and the highest release, shown at 8 h of release time, was approximately 65%. Prolonged release of encapsulated CU may increase the resident time of CU on the skin surface. Also, encapsulation of CU has mostly avoided burst release of CU and avoided high amounts of CU in contact with skin. This property is very significant as any direct contact of the skin with CU that exceeds its toxic limit would be harmful (Krausz *et al*., 2015). Moreover, controlled release of encapsulated CU may avoid the bright yellow pigmentation leading to skin discoloration caused by free CU accumulating on the skin surface.

The release of CU from CU-Al nanoparticles at pH 4.7 was significantly different from the release of CU from CU-Al at pH 5.5. In fact, the maximum release of CU from CU-Al nanoparticles at pH 4.7 was much lower (approx. 27%) than that at pH 5.5 (approx. 65%). This is in accordance with the literature that has shown lower release of encapsulated material in artificial sweat than media of higher pH (Pamunuwa *et al*., 2015). Interestingly, free CU displayed a release pattern almost similar to CU-Al in artificial sweat (pH 4.7). The maximum release of free CU was nearly 35%. Low release of free CU and CU from CU-Al nanoparticles at pH 4.7 may be due to the low solubility of CU in aqueous media of low pH that lead to crystallization and sedimentation of CU (Zheng & McClements, 2020).

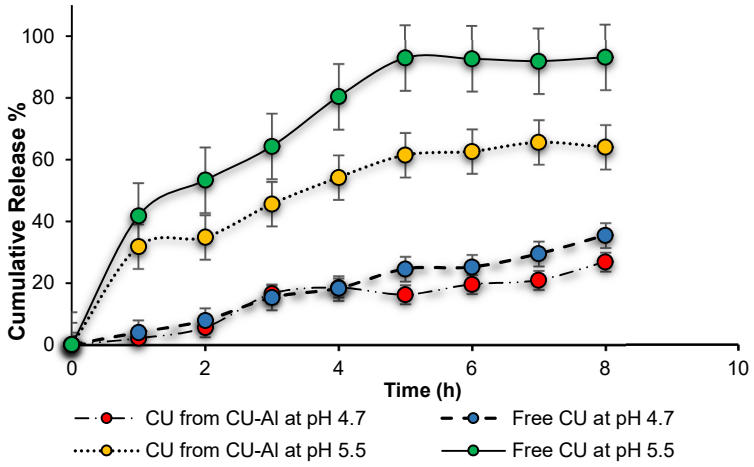

Figure 4: Release of free CU and CU from CU-Al nanoparticles at pH 5.5 and artificial sweat pH 4.7 (CU – free curcumin, CU-Al – Curcumin encapsulated alginate particles)

Further evaluation of the pharmacokinetics of CU release from CU-Al nanoparticles was carried out at skin pH 5.5 and artificial sweat pH 4.7. Table 3 shows the adjusted R^2 values of the release profiles fitted to different kinetic models and the model of best fit was selected based on these values.

At pH 5.5, the Weibull model fitted well with the release profile of CU from the CU-Al spherical nanoparticles confirming that the best release model for swellable polymeric matrix is the Weibull model (Azadi *et al*., 2017). At pH 4.7, the Gompertz and Weibull models described the release of CU from the nanoparticles. Both Weibull and Gompertz models infer a sigmoidal pattern of release of encapsulated CU.

Table 3: Correlation coefficients (adjusted R^2 values) of release kinetic model fitting for CU release from CU-Al nanoparticles at pH 5.5 and pH 4.7 (artificial sweat)

Models n = 3	Release of CU from CU-Al nanoparticles at pH 5.5 Adjusted R^2 values Mean ± SD	Release of CU from CU-Al nanoparticles at pH 4.7 Adjusted R^2 values Mean ± SD
Zero order	0.769 ± 0.040^{b}	0.846 ± 0.011^{a}
First order	0.383 ± 0.026^{c}	0.744 ± 0.029^{a}
Higuchi	0.914 ± 0.022^{a}	0.828 ± 0.052^{a}
Hixson-Crowell	0.360 ± 0.037^{c}	0.476 ± 0.008^{b}
Baker-Lonsdale	0.410 ± 0.070^{c}	0.094 ± 0.348^{c}
Weibull	0.916 ± 0.048^{a}	0.851 ± 0.083^{a}
Gompertz	$0.830 \pm 0.090^{a, b}$	0.869 ± 0.084^{a}

Means that do not share the same superscript in the same column are significantly different ($p < 0.05$).
n: number of trials; CU: curcumin; CU-Al: curcumin encapsulated alginate

Alginate is a water-soluble polymer showing pH-dependent behavior. The release of a bioactive compound from alginate occurs after alginate undergoes hydration, swelling, relaxation of the chains, or erosion. At low pH levels, alginate chains tend to shrink considerably, and with the increase of the pH level, the chains undergo relaxation followed by swelling of the alginate matrix, with an enhancement of the porosity of the structure (Tønnesen & Karlsen, 2002). Considering the aforementioned phenomena, the release of CU from the nanoparticles at pH 5.5 and pH 4.7 could take place due to either pure diffusion, swelling, or polymer erosion/degradation controlled mechanisms. In this regard, obtaining the diffusional coefficient (n value) using the linearized power law equation (equation 12) is essential for a better understanding of the release mechanisms of encapsulated CU at those pHs.

At pH 5.5, the diffusional coefficient (n) value obtained for CU release from nanoparticles was 0.61, which indicated an anomalous transport mechanism. This mechanism is a non-Fickian transport mechanism of which release is governed by a combination of diffusion and chain relaxation (Azad *et al*., 2020). Therefore, the alginate polymer must have undergone a considerable amount of chain relaxation and solvent diffusion to the same extent, leading to polymer swelling, thereby releasing CU at the skin pH of 5.5. Previous studies on alginate hydrogels have concluded that the release of lipophilic bioactive agents (such as curcumin) were controlled by swelling of the hydrogel and diffusion of the bioactives (Xu *et al.,* 2019).

At pH 4.7, the n value was 1.16, which displayed a super case II transport mechanism of encapsulated CU, which indicated a release of CU due to the expansion or relaxation/erosion of alginate chains (El-Houssiny *et al*., 2017; Azad *et al*., 2020). This observation may probably be due to the high NaCl concentration present in artificial sweat medium, which affected the solubility of alginate. That is, Ca^{2+} ions involved in hardening of the alginate matrix via crosslinking, forming a hydrogel structure (Reddy & Nagabhushanam, 2019), may have undergone ion exchange with Na^{+} ions in the solution. During the ion exchange, partial disintegration of the previously insoluble structure may have occurred due to the destabilization of the egg-box structure, leading to higher solubility of the matrix (Segale *et al*., 2016). Despite the fact that rapid release of CU was expected due to rapid polymer relaxation/erosion, the reason for a lower CU release from the nanoparticles at pH 4.7 may be due to the low solubility of CU in the acidic medium. Besides, the similar release pattern observed for free CU at pH 4.7 indicates that the reduced rate of CU release from CU-Al at pH 4.7 may be due to low solubility of CU. It has been found that increased salt (NaCl) concentrations (2-500 mM) influences CU decomposition (Mondal *et al*., 2016). Therefore, poor acidic solubility of CU supported by NaCl concentration of artificial sweat (pH 4.7) may have affected CU solubility and stability in the release medium.

Therefore, considering the overall outcomes, further improvements in engineering of CU-Al nanoparticles may be essential to enhance the solubility of CU, especially in the presence of sweat. However, utilization of nano-encapsulation to facilitate slow release of CU at both skin pH and artificial sweat, could result in enhancement of both skin deposition and skin penetration.

CONCLUSION

Nanoparticles of CU-Al showed properties, especially particle size, PDI, and encapsulation efficiency, favorable for topical skin application. Encapsulation of CU in alginate provided slow controlled release of CU, thus, enabling prolonged release of CU from the nanoparticles so that sustained topical or skin delivery may take place. Also, photodegradation of CU occurring on exposure to sun light (UV rays) could be avoided, especially, when the active ingredient CU encapsulated in alginate is applied on the skin via nanocosmetic formulations. Therefore, encapsulated CU is expected to exhibit greater activity and photo-stability once applied on the skin. However, improving the activity of CU during sweating may require skin deposition or skin penetration of nanoparticles encapsulated with CU mainly due to poor solubility of free CU. Evaluation of both the release model and release mechanism indicated that release of CU at the skin pH and in artificial sweat occurs due to diffusion and polymer expansion respectively, along with chain relaxation and swelling of the particles. However, the extent of skin penetration of free CU and nanoencapsulated CU needs to be evaluated for a better understanding of the overall skin delivery process. Therefore, *in vivo* experiments leading to human clinical trials should be conducted to evaluate the therapeutic effect of curcumin-alginate formulations fabricated in this study for topical application especially during sweating conditions.

Acknowledgement

This work was supported by the (then) Ministry of Science, Technology and Research, Sri Lanka (Grant no: MTR/TRD/AGR/3/2/05). The authors acknowledge the Department of Science and Technology, Faculty of Science and Technology, Uva-Wellassa University, Sri Lanka for allowing the use of the FTIR instrument.

REFERENCES

Aderibigbe B.A. & Buyana B. (2018). Alginate in wound dressings. *Pharmaceutics* **10**(2): 42. DOI: https://doi.org/10.3390/pharmaceutics10020042

Afaq F. & Mukhtar H. (2006). Botanical antioxidants in the prevention of photocarcinogenesis and photoaging. *Experimental Dermatology* **15**: 678–84. DOI: https://doi.org/10.1111/j.1600-0625.2006.00466.x

Ariyarathna I.R. & Karunaratne D.N. (2016). Microencapsulation stabilizes curcumin for efficient delivery in food applications. *Food Packaging and Shelf Life* **10**:79–86. DOI: https://doi.org/10.1016/j.fpsl.2016.10.005

Azad A.K., Al-Mahmood S.M., Chatterjee B., Wan Sulaiman W.M., Elsayed T.M. & Doolaanea A.A. (2020). Encapsulation of black seed oil in alginate beads as a pH-sensitive carrier for intestine-targeted drug delivery: In vitro, in vivo and ex vivo study. *Pharmaceutics* **12**(3):219. DOI: https://doi.org/10.3390/pharmaceutics12030219

Azadi S., Ashrafi H., & Azadi A. (2017). Mathematical modeling of drug release from swellable polymeric nanoparticles. *Journal of Applied Pharmaceutical Science* **7**:125–133. DOI: https://doi.org/10.7324/JAPS.2017.70418

Boonme P., Junyaprasert V.B., Suksawad N. & Songkro S. (2009). Microemulsions and nanoemulsions: Novel vehicles for whitening cosmeceuticals. *Journal of Biomedical Nanotechnology* **5**:373–383. DOI: https://doi.org/10.1166/jbn.2009.1046

Chanchal D. & Swarnlata S. (2008). Novel approaches in herbal cosmetics. *Journal of Cosmetic Dermatology* **7**:89–95. DOI: https://doi.org/10.1111/j.1473-2165.2008.00369.x

Chen X., Zou L.Q., Niu J., Liu W., Peng S.F. & Liu C.M. (2015). The stability, sustained release and cellular antioxidant activity of curcumin nanoliposomes. *Molecules* **20**: 14293–14311. DOI: https://doi.org/10.3390/molecules200814293

Danaei M., Dehghankhold M., Ataei S., Hasanzadeh Davarani F., Javanmard R., Dokhani A., Khorasani S. & Mozafari M. R. (2018). Impact of Particle Size and Polydispersity Index on the Clinical Applications of Lipidic Nanocarrier Systems. *Pharmaceutics* **10**(2): 57. DOI: https://doi.org/10.3390/pharmaceutics10020057

Dash S., Murthy P.N., Nath L. & Chowdhury P. (2010). Kinetic modeling on drug release from controlled drug delivery systems. *Acta Poloniae Pharmaceutica* **67**: 217–23.

De Oliveira R.S., Fantaus S.S., Guillot A.J., Melero A. & Beck R.C.R. (2021). 3D-printed products for topical skin applications: from personalized dressings to drug delivery. *Pharmaceutics* **13**(11): 1946. DOI: https://doi.org/10.3390/pharmaceutics13111946

Dutta A.K. & Ikiki E. (2013). Novel drug delivery systems to improve bioavailability of curcumin. *Journal of Bioequivalence and Bioavailability* **6**:001–9. DOI: http://dx.doi.org/10.4172/jbb.1000172

El-Houssiny A.S., Ward A.A., Mostafa D.M., Abd-El-Messieh S.L., Abdel-Nour K.N., Darwish M.M. & Khalil W.A. (2017). Sodium alginate nanoparticles as a new transdermal vehicle of glucosamine sulfate for treatment of osteoarthritis. *European Journal of Nanomedicine* **9**:105–114. DOI: https://doi.org/10.1515/ejnm-2017-0008

European Pharmacopoeia 7.0 (2021). Buffer Solutions. Available at: https://www.researchgate.net/profile/Samarth_Zarad/post/How_to_prepare_20_mM_sodium_acetate_buffer_pH_46/attachment/59d6526079197b80779aa9b2/AS%3A512087772364801%401499102647435/download/USEPA+_BUFFER.PDF Accessed on 02 Jan 2021.

Guadarrama-Acevedo M.C. *et al.* (14 authors) (2019). Development and evaluation of alginate membranes with curcumin-loaded nanoparticles for potential wound-healing applications. *Pharmaceutics* **11**(8): 389. DOI: https://doi.org/10.3390/pharmaceutics11080389

Hoet P.H., Bruske-Hohlfield I. & Salata O.V. (2004). Nanoparticles-known and unknown health risks. *Journal of Nano biotechnology* **2**:12. DOI: https://doi.org/10.1186/1477-3155-2-12

Ismail E.H., Sabry D.Y., Mahdy H. & Khalil M.M. (2014). Synthesis and characterization of some ternary metal complexes of curcumin with 1, 10-phenanthroline and their anticancer applications. *Journal of Science Research* **6**: 509–519. DOI: https://doi.org/10.3329/jsr.v6i3.18750

Ji J., Wu D., Liu L., Chen J. & Xu Y. (2012). Preparation, characterization, and in vitro release of folic acid-conjugated chitosan nanoparticles loaded with methotrexate for targeted delivery. *Polymer Bulletin* **68**: 1707–1720. DOI: https://doi.org/10.1007/s00289-011-0674-x

Kim, B., Cho, H.E., Moon, S.H., Ahn, H.J., Bae, S., Cho, H.D. & An, S. (2020). Transdermal delivery systems in cosmetics. *Biomedical Dermatology* **4**:1–2. DOI: https://doi.org/10.1186/s41702-020-0058-7

Kim Y.J., Yoon K.J. & Ko S.W. (2000). Preparation and properties of alginate superabsorbent filament fibers crosslinked with glutaraldehyde. *Journal of Applied Polymer Science* **78**: 1797–804.

DOI: https://doi.org/10.1002/1097-4628(20001205)78:10<1797::AID-APP110>3.0.CO;2-M

Korsmeyer R.W., Gurny R., Doelker E., Buri P. & Peppas N.A. (1983). Mechanisms of solute release from porous hydrophilic polymers. *International Journal of Pharmaceutics* **15**: 25–35.
DOI: https://doi.org/10.1016/0378-5173(83)90064-9

Krausz A.E. *et al.* (14 authors) (2015). Curcumin-encapsulated nanoparticles as innovative antimicrobial and wound healing agent. *Nanomedicine* **11**: 195–206.
DOI: https://doi.org/10.1016/j.nano.2014.09.004

Kumari A., Raina N., Wahi A., Goh K.W., Sharma P., Nagpal R. & Gupta M. (2022). Wound-healing effects of curcumin and its nanoformulations: a comprehensive review. *Pharmaceutics* **14**(11): 2288.
DOI: https://doi.org/10.3390/pharmaceutics14112288

Larosa C., Salerno M., de Lima J.S., Meri R.M., da Silva M.F., de Carvalho L.B. & Converti A. (2018). Characterisation of bare and tannase-loaded calcium alginate beads by microscopic, thermogravimetric, FTIR and XRD analyses. *International Journal of Biological Macromolecules* **115**: 900–906.
DOI: https://doi.org/10.1016/j.ijbiomac.2018.04.138

Lee B.H., Choi H.A., Kim M.R. & Hong J. (2013a). Changes in chemical stability and bioactivities of curcumin by ultraviolet radiation. *Food Science and Biotechnology* **22**:279–282.
DOI: https://doi.org/10.1007/s10068-013-0038-4

Lee O., Jeong S.H., Shin W.U., Lee G., Oh C. & Son S.W. (2013b). Influence of surface charge of gold nanorods on skin penetration. *Skin Research and Technology* **19**: e390–e396.
DOI: https://doi.org/10.1111/j.1600-0846.2012.00656.x

Li D., Wu Z., Martini N. & Wen J. (2011). Advanced carrier systems in cosmetics and cosmeceuticals: a review. *Journal of Cosmetic Science* **62**: 549–63.

Mondal S., Ghosh S. & Moulik S.P. (2016) Stability of curcumin in different solvent and solution media: UV–visible and steady-state fluorescence spectral study. *Journal of Photochemistry and Photobiology B: Biology* **158**: 212–218.
DOI: https://doi.org/10.1016/j.jphotobiol.2016.03.004

Nair R.S., Morris A., Billa N. & Leong C.O. (2019). An evaluation of curcumin-encapsulated chitosan nanoparticles for transdermal delivery. *AAPS PharmSciTech* **20**: 1–3.
DOI: https://doi.org/10.1208/s12249-018-1279-6

Nastaj J., Przewłocka A. & Rajkowska-Myśliwiec M. (2016). Biosorption of Ni (II), Pb (II) and Zn (II) on calcium alginate beads: equilibrium, kinetic and mechanism studies. *Polish Journal of Chemical Technology* **8**: 81–7.
DOI: https://doi.org/10.1515/pjct-2016-0052

Nguyen H.T.P., Munnier E., Souce M., Perse X., David S., Bonnier F. & Chourpa I. (2015). Novel alginate-based nanocarriers as a strategy to include high concentrations of hydrophobic compounds in hydrogels for topical application. *Nanotechnology* **26**(25): 255101.
DOI: https://doi.org/10.1088/0957-4484/26/25/255101

Okagu O.D., Verma O., McClements D.J. & Udenigwe C.C. (2020). Utilization of insect proteins to formulate nutraceutical delivery systems: encapsulation and release of curcumin using mealworm protein-chitosan nano-complexes. *International Journal of Biological Macromolecules* **151**: 333–43.
DOI: https://doi.org/10.1016/j.ijbiomac.2020.02.198

Pamunuwa G., Anjalee N., Kukulewa D., Edirisinghe C., Shakoor F. & Karunaratne D.N. (2020). Tailoring of release properties of folic acid encapsulated nanoparticles via changing alginate and pectin composition in the matrix. *Carbohydrate Polymer Technologies and Applications* **1**: 100008.
DOI: https://doi.org/10.1016/j.carpta.2020.100008

Pamunuwa G., Nilakshi H., Rajapaksha G., Shakoor F. & Karunaratne D.N. (2021). Sensory and physicochemical properties and stability of folic acid in a pineapple ready-to-serve beverage fortified with encapsulated folic acid. *Journal of Food Quality* **2021**: 9913884.
DOI: https://doi.org/10.1155/2021/9913884

Pamunuwa G., Karunaratne V. & Karunaratne D. (2016). Effect of lipid composition on in vitro release and skin deposition of curcumin encapsulated liposomes. *Journal of Nanomaterials* **2016**: 4535790.
DOI: https://doi.org/10.1155/2016/4535790

Pamunuwa K.M.G.K., Bandara C.J., Karunaratne V. & Karunaratne D.N. (2015). Optimization of a liposomal delivery system for the highly antioxidant methanol extract of stem-bark of *Schumacheria castaneifolia* Vahl. *Journal of Chemical and Pharmaceutical Research* **7**: 1236–1245.

Paradee N., Sirivat A., Niamlang S. & Prissanaroon-Ouajai W. (2012). Effects of crosslinking ratio, model drugs, and electric field strength on electrically controlled release for alginate-based hydrogel. *Journal of Materials Science: Materials in Medicine* **23**: 999–1010.
DOI: https://doi.org/10.1007/s10856-012-4571-0

Pecora T.M., Cianciolo S., Catalfo A., De Guidi G., Ruozi B., Cristiano M.C., Paolino D., Graziano A.C., Fresta M. & Pignatello R. (2016). Preparation, characterization and photostability assessment of curcumin microencapsulated within methacrylic copolymers. *Journal of Drug Delivery Science and Technology* **33**: 88–97.
DOI: https://doi.org/10.1016/j.jddst.2016.03.013

Peppas N.A. & Sahlin J.J. (1989). A simple equation for the description of solute release. III. Coupling of diffusion and relaxation. *International Journal of Pharmaceutics* **57**: 169–172.
DOI: https://doi.org/10.1016/0378-5173(89)90306-2

Randin J.P. (1987). Pitting potential of stainless steels in artificial sweat. *Materials and Corrosion* **38**: 175–183.
DOI: https://doi.org/10.1002/maco.19870380404

Reddy K.V. & Nagabhushanam M. (2019). Preparation of gastro retentive mucoadhesive beads for atorvastatin by using ionic gelation method with divalence and trivalence curing agents and their characterization studies. *International Journal of Pharmaceutical Sciences and Research* **10**: 157–179.
DOI: https://doi.org/10.13040/IJPSR.0975-8232.10(1).157-79

Rungphanichkul N., Nimmannit U., Muangsiri W. & Rojsitthisak P. (2011). Preparation of curcuminoid niosomes for enhancement of skin permeation. *International Journal of Pharmaceutical Sciences* **66**: 570–575.
DOI: https://doi.org/10.1691/ph.2011.1018

Sahu S. & Mallick B.C. (2022). Curcumin-Alginate mixed nanocomposite: an evolving therapy for wound healing. In: *Properties and Applications of Alginates* (eds. E Deniz, E. Imamoglu & T.K. Gundogdu), pp. **131**. IntechOpen Limited, London, UK.
DOI: https://doi.org/10.5772/intechopen.98830

Saraf S. & Kaur C.D. (2010). Phytoconstituents as photoprotective novel cosmetic formulations. *Pharmacognosy Reviews* **4**:1.
DOI: https://dx.doi.org/10.4103%2F0973-7847.65319

Segale L., Giovannelli L., Mannina P. & Pattarino F. (2016). Calcium alginate and calcium alginate-chitosan beads containing celecoxib solubilized in a self-emulsifying phase. *Scientifica* **2016:** 5062706.
DOI: https://doi.org/10.1155/2016/5062706

Sinico C., Manconi M., Peppi M., Lai F., Valenti D. & Fadda A.M. (2005). Liposomes as carriers for dermal delivery of tretinoin: in vitro evaluation of drug permeation and vesicle–skin interaction. *Journal of Controlled Release* **103**:123–36.
DOI: https://doi.org/10.1016/j.jconrel.2004.11.020

Shakoor I.F., Pamunuwa G.K. & Karunaratne D.N. (2023). Efficacy of alginate and chickpea protein polymeric matrices in encapsulating curcumin for improved stability, sustained release and bioaccessibility. *Food Hydrocolloids for Health*, 100119.
DOI: https://doi.org/10.1016/j.fhfh.2023.100119

Sharma A., Mittal A., Puri V., Kumar P. & Singh I. (2020). Curcumin-loaded, alginate–gelatin composite fibers for wound healing applications. *3 Biotech* **10**(11): 1–13.
DOI: https://doi.org/10.1007/s13205-020-02453-5

Suhail M., Janakiraman A.K., Khan A., Naeem A., & Badshah F.S. (2019). Surfactants and their role in pharmaceutical product development: an overview. *Journal of Pharmacy and Pharmaceutics* **6:** 72–82.
DOI: https://doi.org/10.15436/2377-1313.19.2601

Svobodová A., Psotová J. & Walterová D. (2003). Natural phenolics in the prevention of UV-induced skin damage: a review. *Biomedical Papers* **147**: 137–45.
DOI: https://doi.org/10.5507/bp.2003.019

Taib S.H., Abd Gani S.S., Ab Rahman M.Z., Basri M., Ismail A. & Shamsudin R. (2015). Formulation and process optimizations of nano-cosmeceuticals containing purified swiftlet nest. *RSC Advances* **5**: 42322–42328.
DOI: https://doi.org/10.1039/C5RA03008K.

Thangapazham R.L., Sharad S. & Maheshwari R.K. (2013). Skin regenerative potentials of curcumin. *Biofactors* **39**:141–149.
DOI: https://doi.org/10.1002/biof.1078.

Try C., Moulari B., Béduneau A., Fantini O., Pin D., Pellequer Y. & Lamprecht A. (2016). Size dependent skin penetration of nanoparticles in murine and porcine dermatitis models. *European Journal of Pharmaceutics and Biopharmaceutics* **100**: 101–108.
DOI: https://doi.org/10.1016/j.ejpb.2016.01.002

Tønnesen H.H. & Karlsen J. (2002). Alginate in drug delivery systems. *Drug Development and Industrial Pharmacy* **28**: 621–630.
DOI: https://doi.org/10.1081/DDC-120003853

Tønnesen H.H., Karlsen J. & van Henegouwen G.B. (1986). Studies on curcumin and curcuminoids VIII. Photochemical stability of curcumin. *Zeitschrift für Lebensmittel-Untersuchung und Forschung* **183**:116–122.
DOI: https://doi.org/10.1007/BF01041928

Uchechi O., Ogbonna J.D. & Attama A.A. (2014). Nanoparticles for dermal and transdermal drug delivery. *Application of Nanotechnology in Drug Delivery* **4**:193–227.
DOI: http://dx.doi.org/10.5772/58672.

Usmiati S., Richana N., Mangunwidjaja D., Noor E. & Prangdimurti E. (2014). The using of ionic gelation method based on polysaccharides for encapsulating the macromolecules–a review. *Encapsulation for Protecting the Bioactive Compounds* **67**: 79–84.
DOI: http://dx.doi.org/10.7763/IPCBEE. 2014.V67.16

Xu W., Huang L., Jin W., Ge P., Shah B.R., Zhu D. & Jing, J. (2019). Encapsulation and release behavior of curcumin based on nanoemulsions-filled alginate hydrogel beads. *International Journal of Biological Macromolecules* **134**: 210–215.

DOI: https://doi.org/10.1016/j.ijbiomac.2019.04.200

Zakerikhoob M., Abbasi S., Yousefi G., Mokhtari M. & Noorbakhsh M.S. (2021). Curcumin-incorporated crosslinked sodium alginate-g-poly (N-isopropyl acrylamide) thermo-responsive hydrogel as an in-situ forming injectable dressing for wound healing: In vitro characterization and in vivo evaluation. Carbohydrate Polymers **271**: 118434.

Zamarioli C.M., Martins R.M., Carvalho E.C. & Freitas L.A. (2015). Nanoparticles containing curcuminoids (Curcuma longa): development of topical delivery formulation. *Revista Brasileira de Farmacognosia* **25**: 53–60. DOI: https://doi.org/10.1016/j.bjp.2014.11.010

Zhao Y.Z., Lu C.T., Zhang Y., Xiao J., Zhao Y.P., Tian J.L., Xu Y.Y., Feng Z.G. & Xu C.Y. (2013). Selection of high efficient transdermal lipid vesicle for curcumin skin delivery. *International Journal of Pharmaceutics* **454**: 302–309. DOI: https://doi.org/10.1016/j.ijpharm.2013.06.052

Zheng B. & McClements D.J. (2020). Formulation of more efficacious curcumin delivery systems using colloid science: enhanced solubility, stability, and bioavailability. *Molecules* **25**: 2791. DOI: https://doi.org/10.3390/molecules25122791.